Switching behavior of a Stoner particle beyond the relaxation time limit

M. Bauer, J. Fassbender,* and B. Hillebrands
Fachbereich Physik und Forschungsschwerpunkt Materialwissenschaften, Universität Kaiserslautern, Erwin-Schrödinger-Str. 46, 67663 Kaiserslautern, Germany

R. L. Stamps
Department of Physics, University of Western Australia, Perth, Australia
(Received 4 June 1999)

Results of the switching properties of Stoner-like magnetic particles, subject to short magnetic field pulses, obtained by numerical investigations, are reported. The switching properties are discussed as a function of the external field pulse strength and direction, pulse length, and the pulse shape. For field pulses long compared to the precession time, the switching behavior is governed by the magnetic damping term. In the limit of short field pulses, switching properties are dominated by the details of the magnetic precession. In the latter case, the magnetic damping term is of minor importance and ultrafast switching can be achieved by choosing the right field pulse parameters. It is also possible to choose pulse parameters in order to provide switching over a wide range of applied field directions.

I. INTRODUCTION

Magnetization reversal in magnetic particles is one of the fundamental issues in magnetic data storage. Current and perspective technologies require understanding and controlling dynamic magnetization processes in fine particles on nanosecond time scales. This is an interesting region to study because the dynamic processes are highly nonlinear in this regime.

Because of advances in nanoscale lithographic techniques, and the current ability to shape submicron sized magnetic particles with great precision, a huge variety of experimental geometries are possible. To date, only a restricted number of special cases have been examined, and only for a narrow range of magnetic-field configurations.[1–4]

Useful models for the switching process can be formulated as semiclassical Landau-Lifschitz equations of motion with a Gilbert damping term. For a static applied field, switching by the homogeneous rotation of the magnetization or nucleation and propagation of domain walls, and combinations thereof, have been studied thoroughly.[1,4,5] Initial work on precession dominated reversal of Stoner particles in static fields was discussed in detail by Brown,[6] and recent work has begun probing this region experimentally.[7,8]

Pulsed field reversal is less well studied. Precession effects can be expected to be particularly important on time scales where the length of the field pulse is comparable or shorter than the typical relaxation time of the magnetization. In this region, the strength, duration, and direction of the applied field pulse are important.

The purpose of this paper is to examine details of the reversal process, calculated for single domain ellipsoidal particles, under a variety of different reversal field configurations. In particular, the effects on high-speed switching of magnetic-field pulse duration, strength, and orientation are simulated. A practical method of analysis is proposed.

The following studies are relevant to reversal processes in isolated single domain magnetic particles with homogeneous magnetization. The present results apply to the switching properties of individual small magnetic grains in a data storage medium, sensors, and magnetic random access memory (MRAM) cells with small geometries.

II. MODEL

Shape anisotropy in the magnetic particle can be described by demagnetization factors in the x, y, and z direction, N_x, N_y, and N_z. Only ellipsoidally shaped particles and infinite films are considered, so that the demagnetization field is assumed constant across the sample. All calculations presented in the following are performed for permalloy [saturation magnetization $4\pi M_S = 10.8$ kG, gyromagnetic factor $\gamma = 0.0176\ \mathrm{Oe}^{-1}\,\mathrm{ns}^{-1}$, and the Gilbert magnetic damping factor $\alpha = 0.008$ (Refs. 7 and 9)]. Only shape and uniaxial in-plane anisotropies are considered. Except for the sphere case, the demagnetization factors or the anisotropy field are chosen such that the equilibrium magnetization direction, under zero applied field conditions, lies in the xy plane (in-plane). For all anisotropies the x axis corresponds to the easy axis of magnetization. In all cases, the initial magnetization direction is taken to be along the negative x direction.

The motion of the magnetization under the influence of an effective magnetic field and with a phenomenological damping may be described by the Gilbert form of the Landau-Lifschitz equation[10–12]

$$\frac{\partial \vec{M}}{\partial t} = -\gamma \vec{M} \times \vec{H}_{eff} + \frac{\alpha}{M_S} \vec{M} \times \frac{\partial \vec{M}}{\partial t}. \tag{1}$$

The first term on the right-hand side is the precession term and the second one is the damping term. The effective field $\vec{H}_{eff}$ is defined as the sum of all fields acting on the magnetization

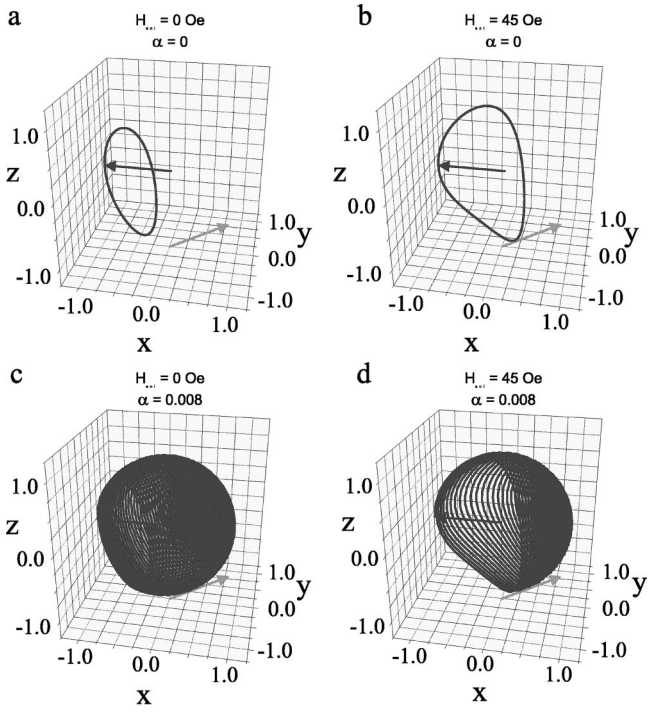

FIG. 1. Time evolution of the magnetization vector of a permalloy sphere. The initial direction of magnetization is along the negative x direction (black arrow); a field of 50 Oe (gray arrow) is applied at an angle of 135° in the xy plane. The time evolution is shown for the first 500 ns. (a) No anisotropy, no damping, (b) uniaxial anisotropy field 45 Oe, no damping, (c) no anisotropy, damping parameter $\alpha=0.008$, and (d) uniaxial anisotropy field 45 Oe, damping parameter $\alpha=0.008$.

$$\vec{H}_{eff}=\vec{H}_{ext}+\vec{H}_{ani}+\vec{H}_{shape},$$

$$\vec{H}_{ani}=|\vec{H}_{ani}|\frac{M_x}{M_S}\hat{x}, \tag{2}$$

$$\vec{H}_{shape}=-(4\pi N_x M_x\hat{x}+4\pi N_y M_y\hat{y}+4\pi N_z M_z\hat{z}),$$

with $\vec{H}_{ext}$ the external applied field, $\vec{H}_{ani}$ the uniaxial in-plane anisotropy field with x the easy axis of magnetization, $N_i(i=x,y,z)$ the diagonal components of the demagnetization tensor in diagonal form, and M_x, M_y, and M_z the vectorial magnetization components along the x,y, and z axes. The results are obtained by numerical integration of Eq. (1) using a standard, self-optimizing, embedded Runge-Kutta algorithm.[13]

III. PRECESSION EFFECTS IN REVERSAL

A. Reversal of an isotropic sphere

In this section, the effects of the shape and uniaxial in-plane anisotropies on the switching behavior are examined. We begin by studying reversal of an isotropic sphere by instantaneously increasing a magnetic field, initially at zero, to a finite, constant value. The magnetic field lies in the xy plane with an angle of 135° with respect to the initial direction of $\vec{M}$. The demagnetization factors of the isotropic sphere are $N_x=N_y=N_z=1/3$.

Figure 1 shows the trajectories of the end point of the magnetization vector in three dimensions for various damping/anisotropy combinations. In all cases, the initial direction of the magnetization lies along the negative x direction, and a field of $H_{ext}=50$ Oe (gray arrow) is applied at time $t_0=0$. The initial magnetization orientation is indicated by the black arrow.

In the absence of damping or anisotropy, the Zeeman energy of the magnetization remains constant and the magnetization will precess in a circular orbit with its plane perpendicular to $\vec{H}_{ext}$, as displayed in Fig. 1(a). Note that no switching can occur without dissipation. If the external field is switched off at time $t_1>t_0$, the magnetization will simply stop at whatever position $\vec{M}$ is in at t_1.

If a uniaxial anisotropy ($H_{ani}=45$ Oe) is present, the orbit of the magnetization becomes elliptical since the effective field is now anisotropic. This is illustrated in Fig. 1(b). Note that the trajectory of the magnetization vector does not lie in a single plane. In this case, if the external field is switched off at time t_1, and if the magnetization is not along an easy direction at that time, then the magnetization will continue to precess about the axis of the anisotropy.

Next the above calculations are repeated for a small damping parameter of $\alpha=0.008$. First, the case of a sphere without uniaxial anisotropy is considered. The trajectory in Fig. 1(c) shows the time evolution of the magnetization during the first 500 ns. The switching of the magnetization occurs because energy is dissipated, thus allowing the magnetization to relax into a low-energy configuration by aligning in the direction of the effective field.

With this small value of the damping parameter, 500 ns are not sufficient to align the magnetization parallel to the applied field. If a uniaxial anisotropy is included, as shown in Fig. 1(d), the switching time is decreased and after 500 ns the magnetization is completely reversed. Note that this result cannot be achieved by increasing the magnitude of the applied field, and is instead due to a deformation of the trajectory.

B. Reversal of an infinite thin film

The effect of shape anisotropy is now examined. We consider an infinite thin film with demagetization factors $N_x=N_y=0$, and $N_z=1$, so that the film is in the xy plane. The results are displayed in Fig. 2. The magnetization is initially aligned along the negative x direction, prior to the application of an external field of 50 Oe. Since the external field is applied in the film plane, the precession orbit is mostly out of the film plane, and hence a significant demagnetization field will appear. Similar to the case of a sphere with uniaxial anisotropy, the precession orbit is strongly deformed. In this case, the anisotropy is an easy plane type, and the magnetization remains close to the film plane.

The orbit shown in Fig. 2(a) consists of two arclike sections almost parallel to the film plane. Note that the magnetization precesses through a large range of in-plane angles. If a uniaxial anisotropy field of 45 Oe is included, the range of in-plane magnetization angles is reduced. This case is shown in Fig. 2(b).

Reversal is possible if the magnetization crosses the hard in-plane axis at some point during its trajectory. This is possible even with very small applied fields. For example, with

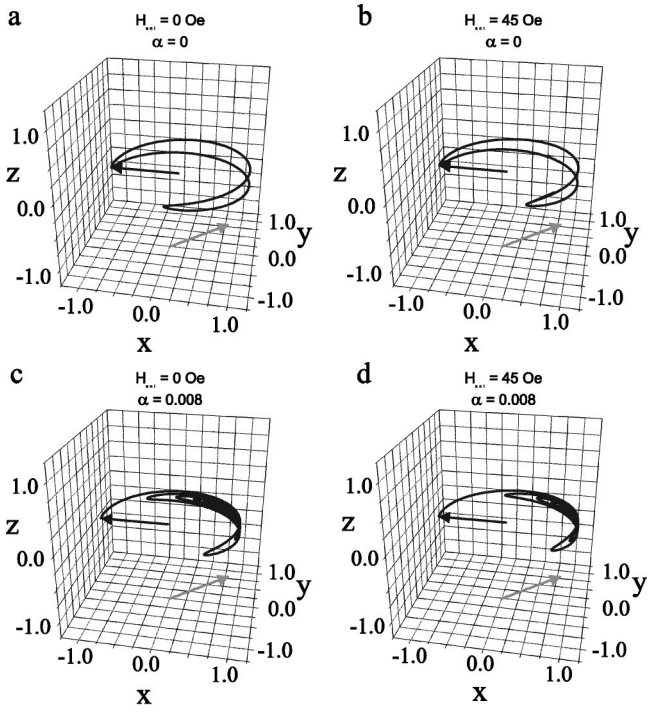

FIG. 2. Time evolution of the magnetization vector of a thin infinitely extended magnetic permalloy film. The time evolution is shown for the first 10 ns. All other parameters are as in Fig. 1.

the parameters used in this study, reversal can be achieved with a field as small as 18 Oe. The influence of damping does not alter this feature. This is shown in Fig. 2(c) for the case of no uniaxial in-plane anisotropy. The magnetization reverses into the direction of the applied field within 5 ns for a field magnitude of 50 Oe. An in-plane uniaxial anisotropy [Fig. 2(d)] also supports reversal inside 5 ns, but the magnetization aligns in this case along the direction of the effective field.

In summary, precession dominated reversal between in-plane orientations can be very fast in the case of a film with an in-plane uniaxial anisotropy. The reason is that the precession frequency is large, so that precession times are short, due to the large shape anisotropy field. This allows very fast reversal from one in-plane orientation to another, because the effective field is mostly perpendicular to the film plane, thus forcing precession to be mostly in-plane.

IV. PRECESSION OF THE MAGNETIZATION IN A PULSED APPLIED FIELD

In this section, switching phenomena under application of a short magnetic-field pulse are discussed. To define the notation of the pulse rise time, pulse length, and pulse fall time used throughout this article, a scheme is outlined as shown in Fig. 3. The pulse is characterized by the triplets of numbers ''rise time/pulse length/fall time.'' For the pulse rise and fall a sinusoidal time dependence is assumed. All values are given in units of nanoseconds.

In Fig. 4 different scenarios of the magnetization switching including damping, initiated by a 0.2/1.0/0.2 magnetic field pulse, are shown. For a film geometry results without in-plane uniaxial anisotropy are shown in (a) and with in-plane uniaxial anisotropy in (b). All parameters except the shape of the pulse are the same as those used to generate Figs. 2(c) and (d). Figures 4(c) and (d) contain the corresponding results for an ellipsoidally shaped particle with the demagnetization factors of $N_x=0.008$, $N_y=0.012$, and $N_z=0.980$. As in Sec. III, the initial direction of magnetization, represented by the black arrow, lies along the negative x

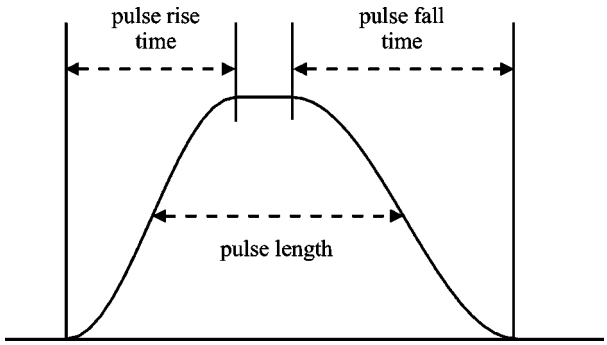

FIG. 3. Scheme of the magnetic-field pulse to explain the parameters pulse rise time/pulse length/pulse fall time. All values are given in units of nanoseconds. Rise and fall times have a sinusoidal shape, and the pulse length is determined as the full width at half maximum.

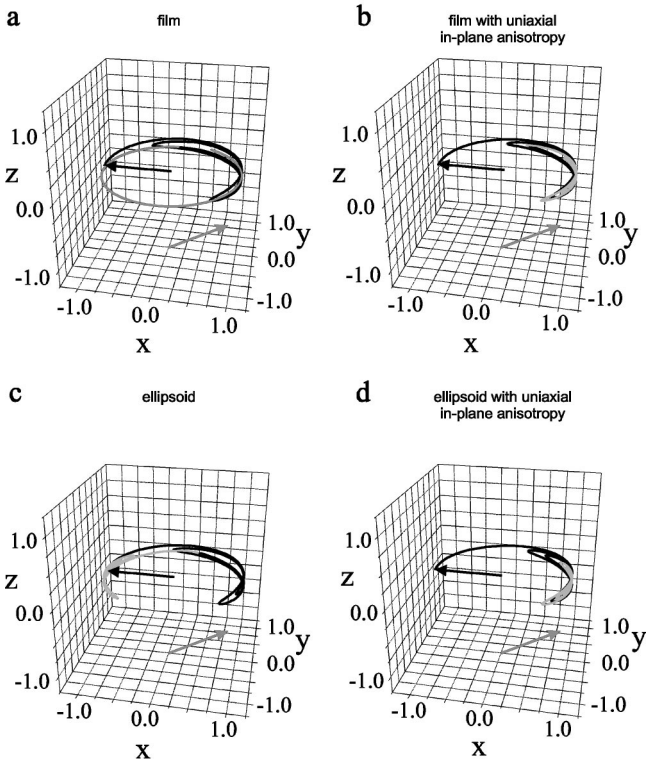

FIG. 4. Different scenarios of the magnetization switching initiated by a 0.2/1.0/0.2 magnetic-field pulse, shown for a thin film without (a) and with (b) anisotropy ($H_{ani}=45$ Oe). (c) and (d) show the corresponding results for an ellipsoidally shaped particle with the demagnetization factors of $N_x=0.008$, $N_y=0.012$, and $N_z=0.980$. The initial direction of magnetization is along the negative x direction (black arrow); a field of 50 Oe (gray arrow) is applied at an angle of 135° in the xy plane. The time evolution is shown for the first 10 ns. Data are represented black (gray) during (after) the magnetic-field pulse.

direction; a field of 50 Oe (gray arrow) is applied at an angle of 135° in the xy plane. The time evolution is shown for the first 10 ns. In these figures, the data during field pulse are represented by black lines, and after the field pulse by gray lines.

In the case of a film without anisotropies, as shown in Fig. 4(a), the magnetic field pulse leads to a damped precession about the effective field direction. When the applied field terminates, the effective field is entirely due to the demagnetization field, and the magnetization precesses in a circular trajectory with a small component initially out of plane. Since no in-plane anisotropy is present, all in-plane angles of the magnetization can be realized as a final state by field pulse length variation.

A uniaxial in-plane anisotropy is included in the calculation and shown in Fig. 4(b). The time evolution of the magnetization during the field pulse is similar to Fig. 4(a). The effective field is modified by the in-plane anisotropy field. The relaxation of the magnetization leads to the final easy magnetization direction, which is closer to the magnetization direction when the pulse was terminated. As discussed below, the final position turns out to be very sensitive to the pulse strength in certain orientations.

In Figs. 4(c) and (d), the demagnetization factor is such, that its in-plane component is comparable in magnitude to the uniaxial in-plane anisotropy. This changes the switching behavior. In the case without anisotropy, the magnetization ultimately rests at its initial position after termination of the field pulse. For this reduced shape anisotropy, the precession time is also reduced, allowing the magnetization to remain in the $x<0$ half space for a long time during the pulse. This increases the probability of relaxing back into the initial direction when the pulse ends.

Figure 4(d) shows the time evolution of the magnetization reversal for an ellipsoidally shaped geometry with a uniaxial anisotropy. Although the resulting in-plane anisotropy contribution is ≈90 Oe, fast and stable switching occurs for a field pulse of 50 Oe.

It is clear from Figs. 4(b) and (c), that the length of the short pulse determines the final state of the magnetization. It should be noted that experimental evidence for this was recently demonstrated by Back *et al.*,[8] testing the domain structure written into a perpendicularly magnetized film by a pulse of high-energy electrons propagating at near speed of light in the Stanford Linear Accelerator Facility. In their experiments it was possible to observe the different domain patterns created by different magnetic-field pulse magnitudes.

V. MAGNETIZATION SWITCHING OF SMALL PARTICLES

For reversal processes we are mainly interested in the final state of the magnetization. As suggested above, the final state is sensitive to the parameters describing the pulse. We suggest here a particular graphical representation that is useful for providing the final configurational state information as a function of the pulse field strength and direction. The representation is shown in Figs. 5 and 6. The ellipsoidally shaped magnetic particle has demagnetization factors $N_x=0.008$, $N_y=0.012$, and $N_z=0.980$. No further anisotropy is considered. The magnetic damping parameter is chosen to $\alpha=0.008$. Prior to the field pulse, the magnetization lies along the negative x direction, and reversal is into the positive x direction. Dark (bright) areas indicate that the final state of magnetization is in the negative (positive) x direction. The circular polar coordinates represent the direction and strength of the field pulse. The strength is zero at the center, and its increment is 25 Oe between circles. The direction from the center indicates the direction of the external field.

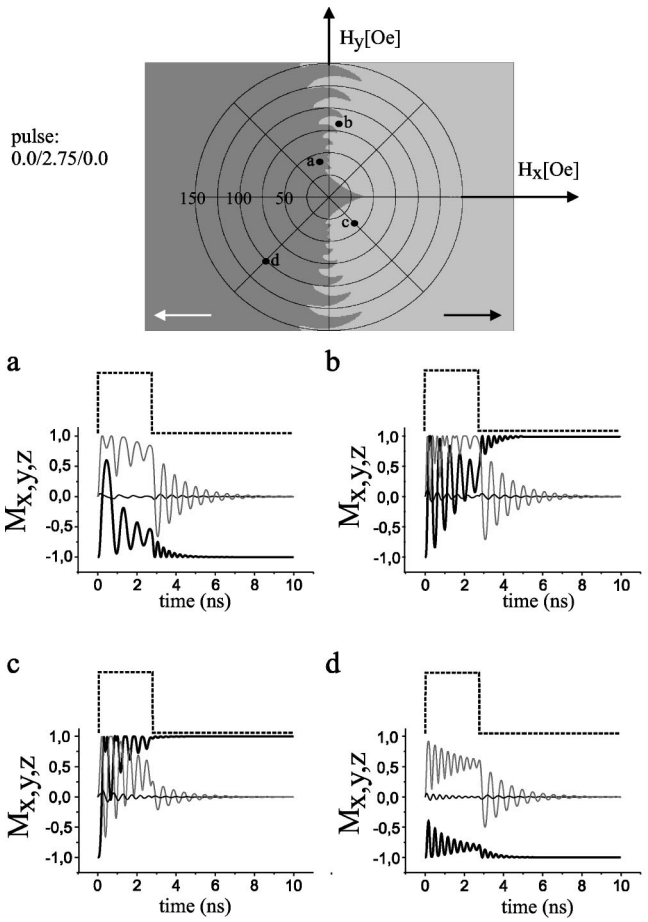

FIG. 5. Switching diagram of an ellipsoidally shaped particle with the demagnetization factors $N_x=0.008$, $N_y=0.012$, and $N_z=0.980$, i.e., the x axis is the easy magnetization axis. The initial direction of magnetization is along the negative x direction. A field pulse of 0/2.75/0 ns is applied. Bright (dark) areas indicate that the magnetization has switched (not switched) from the negative into the positive x direction. The direction of each point of the diagram from the center indicates the direction of the applied field pulse. The strength of the field pulse is proportional to the distance from the center. The circles show increments of the field strength of 25 Oe. The four panels display the time evolution of the three magnetization components M_x (bold black line), M_y (thin gray line), and M_z (thin black line) at the positions indicated in the switching diagram. The time structure of the applied field pulse is shown by the dashed line.

A. Switching with long pulses—the relaxation dominated switching regime

We now apply a 0.0/2.75/0.0 pulse to the ellipsoid. The result is displayed in Fig. 5. It is evident that reversal takes

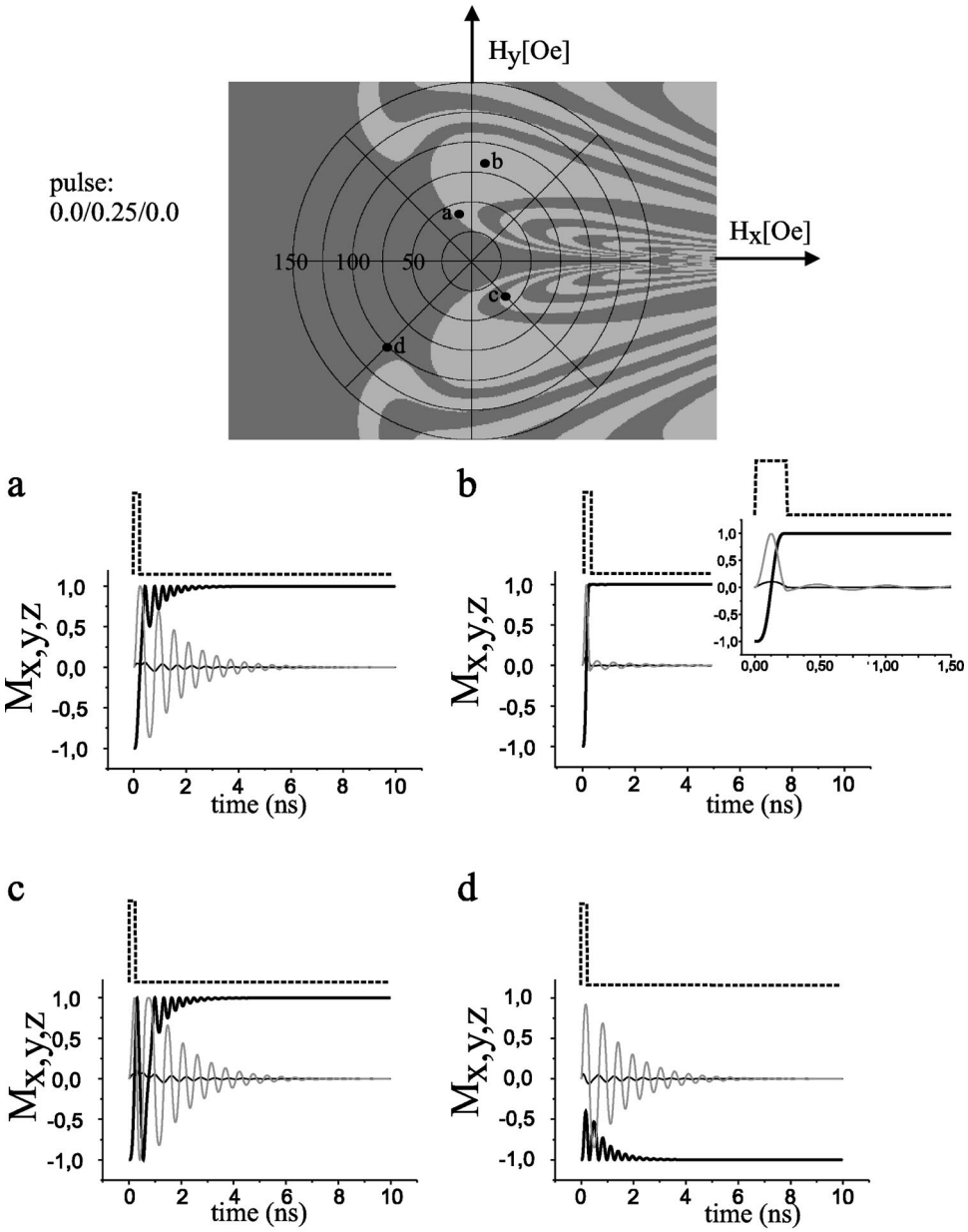

FIG. 6. Switching diagram for a field pulse of 0/0.25/0. All other parameters are as in Fig. 5.

place for most of the parameter sets, where the field direction has a component along the positive x direction. If the field is aligned near the $\pm y$ directions, switching and nonswitching areas alternate with increasing field strength. Along these directions the final configuration is very sensitive to pulse magnitude, and we call this the ''instability region.'' This region exists because during precession about the field in y directions, the x component of the magnetization oscillates between the positive and negative x directions. The final state is determined by the position of the magnetization when the field pulse is terminated. The instability region is due to a beating between the applied field pulse and the precession of the magnetization. Note that if the value of the applied field is too small, no switching will appear.

Note that the angular extent of the instability region increases with field strength. A corresponding increase in the precession frequency increases the angular range covered during precession, and thus extends the instability region.

The four diagrams labeled (a) to (d) in Fig. 5 show the time evolution of all components of the magnetization. Values are shown as a function of time for different field strengths and directions. A significant ''ringing'' of the magnetization at the beginning and ends of the applied field pulse is observed. In all cases the crucial parameter for the switching is the magnetic damping parameter. If the applied field pulse has a component along the positive x direction, damping helps the reversal because the average of the x component can move toward the positive x direction in a single oscillation period. This can be seen in the black lines shown in Figs. 5(b) and (c). Otherwise, damping actually hinders switching because the negative x direction is favored.

B. Switching with short pulses—the precession dominated switching regime

Application of a very short, 0/0.25/0, field pulse is now examined. For moderate applied fields, this pulse length is shorter than the precession period of the magnetization. Figure 6 shows the results of the calculations. Compared to the results of long pulses (cf. Fig. 5) we observe a strongly al-

ternating behavior in the right part of the diagram, where the x component of the applied field is antiparallel to the initial direction of the magnetization. We also find that the regions in the left part of the diagram, where switching can occur, are greatly enlarged. Diagrams 6(a)–(d) illustrate the time evolution of the switching process for the same values and directions of the external field, as in Fig. 5. The final state of the magnetization of Figs. 6(b)–(d) is the same as in Figs. 5(b)–(d). In Fig. 6(a) the magnetization is reversed in contrast to the case shown in Fig. 5(a). This is because the duration of the pulse is short enough to avoid the relaxation into the negative x direction.

A remarkable situation is shown in Fig. 6(b). Full reversal of the magnetization is achieved within the pulse length without significant ringing afterwards. The reason is that the pulse is switched off at the time the z component of the magnetization crosses zero. This is energetically favorable since at this point most of the energy is contained in the Zeeman term which will be dismissed upon field termination. The suppression of the ringing is important for ultrafast applications in order for consecutive pulses to be applied to the same cell without dead time.

VI. INFLUENCE OF THE SHAPE OF THE MAGNETIC FIELD PULSE ON THE MAGNETIZATION REVERSAL

The influence of the pulse shape on the switching properties is summarized in Fig. 7. On the left we show diagrams for rectangularly shaped pulses. In the top figure, the pulse length is 0.25 ns, so that switching is dominated by precession (cf. Fig. 6). In the bottom figure, the pulse length is 2.75 ns, and switching is determined by the relaxation time (cf. Fig. 5). The middle figure shows an example out of the transition region between the precessional and relaxation limits for a pulse length of 1.4 ns.

The right panels of Fig. 7 show the switching diagrams for the same pulse lengths as in the left panels, but with rise and fall times equal to the pulse length. In each case, regions of stable switching into the positive x direction are enlarged compared to the case of a rectangular pulse of same duration, especially for the transition regime. In addition, we find that the angular range of no switching regions (i.e., into the negative x direction) is larger. Hence we find for the bottom right panel a clear separation between the switching and nonswitching areas at the $\pm y$ direction, with the exception of the Stoner asteroid in the center of the diagram for small applied fields.

VII. APPLICATIONS

Criteria for fast and stable switching are derived, and a diagrammatic representation, suggested for analysis, has been presented. We believe that these kind of diagrams may be useful for optimizing switching times in magnetic devices. In particular, this analysis can be used for MRAM storage cell geometries, which usually consist of a magnetic multilayer stack containing the storage element and the sensor structure for readout. Reversal can be achieved using two crossing, current-carrying wires to address and switch the cell. The wires are perpendicular to each other, and aligned

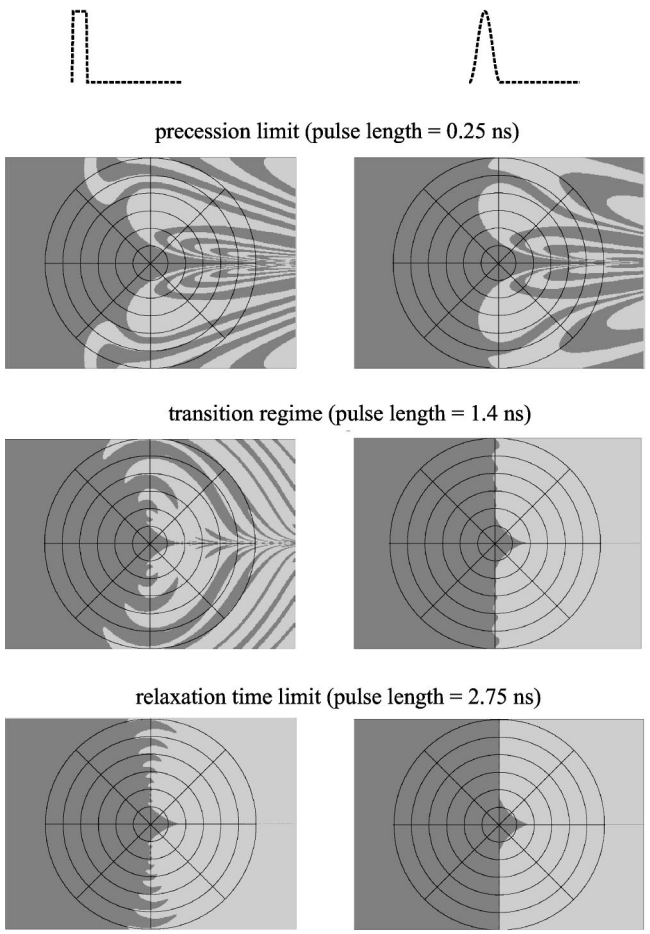

FIG. 7. Switching diagrams as in Figs. 5 and 6 for pulse lengths of 0.25 ns (top), 1.40 ns (middle), and 2.75 ns (bottom). The left panels show the diagrams for rectangularly shaped pulses, the right panels for pulses with rise and fall times equal to the pulse length.

parallel and perpendicular to the easy axis of the storage elements. Each wire alone is supposed not to switch any storage elements. Only the addressed element beneath two current carrying wires will be switched. From Fig. 5, for example, crucial information is extracted about the switching by drawing a square (for identical values of current in each wire) or a rectangle (for different values of current in each wire) around the center. The intersections with the x and y axis contain the information about a possible switching of elements beneath each wire. For stable operation, the intersections with the x and y axis should not switch, but the corner position should indicate successful switching.

To achieve stable switching, for example, for a given range of fluctuations in material parameters, a fairly large range in the diagrams must be considered, where switching occurs. In the precession dominated case, such an area is identified along the $\pm y$ directions. Improved switching of an MRAM memory cell could be achieved by simultanously addressing two data lines which are oriented parallel to the easy axis of magnetization such that the generated field is oriented along the $\pm y$ directions.

VIII. SUMMARY

The switching properties of Stoner-like magnetic particles upon application of short magnetic pulses have been pre-

sented. Switching depends largely on the pulse length and the pulse shape. Two distinct switching mechanisms can be realized. For short field pulses the switching properties are governed by the precession of the magnetization, whereas for long field pulses only the damping term is important. We have shown that by choosing optimum field pulse parameters the damping term is of minor importance and ultrafast switching becomes possible.

ACKNOWLEDGMENTS

We would like to thank R. Lopusnik and C. E. Patton for critically reading the manuscript. Support by Siemens AG, the German ministry of research and technology (BMBF), and the European Union (TMR project Dynaspin) is gratefully acknowledged. R.L.S. thanks the ARC for support.

*Author to whom correspondence should be addressed. Electronic address: fassbend@physik.uni-kl.de

[1] R. Kikuchi, J. Appl. Phys. **27**, 1352 (1957).
[2] L. He, W.D. Doyle, and H. Fujiwara, IEEE Trans. Magn. **30**, 4086 (1994).
[3] W.D. Doyle, S. Stinnet, C. Dawson, and L. He, J. Magn. Soc. Jpn. **22**, 91 (1998).
[4] A. Hubert and R. Schäfer, *Magnetic Domains* (Springer-Verlag, Berlin, 1998).
[5] A. Aharoni, *Introduction to the Theory of Ferromagnetism* (Claredon Press, Oxford, 1996).
[6] W.F. Brown, Jr., Phys. Rev. **130**, 1677 (1963).
[7] M.R. Freeman, W. Hiebert, and A. Stankiewicz, J. Appl. Phys. **83**, 6217 (1998).
[8] C.H. Back, D. Weller, J. Heidmann, D. Mauri, D. Guarisco, E.L. Garwin, and H.C. Siegmann, Phys. Rev. Lett. **81**, 3251 (1998).
[9] C.E. Patton, Z. Frait, and C.H. Wilts, J. Appl. Phys. **46**, 5002 (1975).
[10] L. Landau, and E. Lifschitz, Phys. Z. Sowjetunion **8**, 153 (1953).
[11] T.L. Gilbert, Phys. Rev. **100**, 1243 (1955).
[12] J.C. Mallinson, IEEE Trans. Magn. **23**, 2003 (1987).
[13] J.R. Dormand, and P.J. Prince, J. Comput. Appl. Math. **7**, 67 (1981).